Sensitivity of Linear Models of the Madden–Julian Oscillation to Convective Representation

ŽELJKA FUCHS-STONE[a] AND KERRY EMANUEL[b]

[a] *Climate and Water Center, New Mexico Institute of Mining and Technology, Socorro, New Mexico*
[b] *Lorenz Center, Massachusetts Institute of Technology, Cambridge, Massachusetts*

(Manuscript received 16 June 2021, in final form 9 February 2022)

ABSTRACT: Two analytical models with different starting points of convective parameterizations, the Fuchs and Raymond model on one hand and the Khairoutdinov and Emanuel model on the other, are used to develop "minimal difference" models for the MJO. The main physical mechanisms that drive the MJO in both models are wind-induced surface heat exchange (WISHE) and cloud–radiation interactions (CRI). The dispersion curves for the modeled eastward-propagating mode, the MJO mode, are presented for an idealized case with zero meridional wind and for the realistic cases with higher meridional numbers. In both cases, the two models produce eastward-propagating modes with the growth rate greatest at the largest wavelengths despite having different representations of cumulus convection. We show that the relative contributions of WISHE and CRI are sensitive to how the convection and entropy/moisture budgets are represented in models like these.

SIGNIFICANCE STATEMENT: The Madden–Julian oscillation is the largest weather disturbance on our planet. It propagates eastward encompassing the whole tropical belt. It influences weather all around the globe by modulating hurricanes, atmospheric rivers, and other phenomena. Numerical models that forecast the Madden–Julian oscillation need improvement. Here we explore the physics behind the Madden–Julian oscillation using simple analytical models. Our models are based on the assumption that surface enthalpy fluxes and cloud–radiation interactions are responsible for the Madden–Julian oscillation but it should be borne in mind that other physical mechanisms have been proposed for the MJO. The impact of this research is to better understand the Madden–Julian oscillation mechanism.

KEYWORDS: Cloud radiative effects; Convective-scale processes; Surface fluxes; Thermodynamics; Water vapor

1. Introduction

The Madden–Julian oscillation (MJO) is the largest weather disturbance on our planet, but was only discovered in 1971 by Madden and Julian (Madden and Julian 1971) based on observations of winds and pressure between Singapore and Canton Island in the west-central equatorial Pacific. [A study published in Chinese in 1963 also documented a 40–50-day oscillation in the Asian monsoon region (Xie et al. 1963; Li et al. 2018).] Today we know that even though the MJO is a tropical disturbance, it influences weather all around the globe, modulating hurricanes, atmospheric rivers, and other phenomena (Zhang 2013).

Wheeler and Kiladis (1999) and Kiladis et al. (2009) find, based on wavenumber–frequency power spectra of outgoing longwave radiation (OLR), that the strongest disturbance in OLR in the tropical atmosphere is the MJO. This disturbance propagates eastward with planetary wavenumbers $l = 1, 2$ with a period of about 30–90 days or, for the planetary wavenumber $l = 1$, with phase speeds in the range from 5 to 15 m s^{-1}.

Theoretical modeling of large-scale disturbances in the tropics started with Matsuno (1966), who developed an analytical shallow-water model for the adiabatic atmosphere, i.e., with no convective coupling. The only modes that propagate eastward are the Kelvin mode, higher-order gravity modes, and eastward branch of mixed Rossby–gravity mode in the antisymmetric component of OLR. Researchers after Matsuno (Wheeler and Kiladis 1999; Raymond and Fuchs 2007; Kuang 2008; Kiladis et al. 2009) found that the slower Kelvin waves, when convectively coupled, have largest growth rates for wavenumbers five to seven and that they have vertical structure that differs from that of the MJO. Since the MJO has different scale and structure from the Kelvin mode, it appears not to have an equivalent in a dry atmosphere. This implies that the MJO can exist only when there is moist convection. The modeled mode, if it is the MJO, thus needs to be a convectively coupled mode that has the greatest instability for largest wavelengths and it needs to propagate eastward. This might seem simple, but five decades of research have shown that these are difficult conditions to meet.

Many theoretical models that have tried to explain the mechanisms behind the MJO are well summarized in review papers by Zhang (2005) and by Jiang et al. (2020). Jiang et al. (2020) identifies seven contemporary theories that explain the slow eastward propagation and planetary scale of the MJO. Those are the weak temperature gradient approximation (WTG) moisture mode (Sobel and Maloney 2012, 2013; Adames and Kim 2016), wind-induced surface heat exchange (WISHE) moisture mode (Fuchs and Raymond 2005, 2017; Fuchs-Stone 2020), boundary layer quasi-equilibrium (BLQE)

Denotes content that is immediately available upon publication as open access.

Corresponding author: Željka Fuchs-Stone, zeljka.fuchs@nmt.edu

DOI: 10.1175/JAS-D-21-0165.1

model (Khairoutdinov and Emanuel 2018; Emanuel 2020), trio interaction (Wang and Rui 1990; Wang et al. 2016), skeleton (Majda and Stechmann 2009; Thual et al. 2014), gravity wave (Yang and Ingersoll 2013, 2014), nonlinear solitary wave (Yano and Tribbia 2017; Rostami and Zeitlin 2019), and large-scale convective vortex (Hayashi and Itoh 2017) theories. Four of those theories (skeleton, WTG–moisture mode, gravity wave, and trio-interaction theory) are discussed and compared in detail in a review paper by Zhang et al. (2020). The moisture-mode theory is further discussed in a review paper by Adames and Maloney (2021). Readers are encouraged to read those papers to gain insights into the extensive research on the MJO over the past 50 years.

In this paper we aim to find a common framework between the WISHE-moisture mode and the BLQE models by developing the simplest possible linear analytical model with minimal differences. Those theoretical models are the ones from Fuchs and Raymond (2005, 2017) and Fuchs-Stone (2020) on the one hand and Khairoutdinov and Emanuel (2018) and Emanuel (2020) on the other. The first we will call the FR model and second the KE model. The value of linear analytical models is in their ability to clearly identify the physical mechanism responsible for the instability and propagation mechanism of the MJO. The disadvantage is that the simple analytical models cannot capture nonlinearity or other complexities of the real world.

Two processes that are crucial to the WISHE–moisture mode and the BLQE theories of tropical intraseasonal variability are surface enthalpy fluxes and cloud–radiation effects. We therefore focus on those two mechanisms in comparing the models.

In formulating this paper we take advantage of the fact that there are easterly global mean zonal winds always present in the tropics (Peixoto and Oort 1992; Sentić et al. 2020). We do not view the global (wavenumber 1) MJO as a disturbance occurring only over the warm pool where there are often westerlies (Sobel and Maloney 2012, 2013; Adames and Kim 2016), but rather assume mean easterlies in formulating wind-induced perturbations to the surface enthalpy flux, a process known as WISHE. The WISHE parameterization goes back to Emanuel (1987), Neelin et al. (1987), and Yano and Emanuel (1991) and relies on the fact that mean surface easterly anomalies result in enhanced surface fluxes in the presence of mean easterly winds. Under this paradigm WISHE is responsible for the eastward propagation of the MJO. Sentić et al. (2020) showed the importance of WISHE for the reanalysis-derived climatological MJO through analysis of zonal wind, moisture, and moisture tendency anomalies from reanalyses. The WISHE assumption is challenged by studies that show the surface latent heat fluxes to the east of enhanced MJO convection to be suppressed due to mean westerlies in warm pool (Zhang 1996; Kiranmayi and Maloney 2011; Sobel et al. 2014; de Szoeke et al. 2015). Things get more complicated when we look at the Shi et al. (2018) and Khairoutdinov and Emanuel (2018) aquaplanet simulations that find that suppressing WISHE eliminates the MJO, while the same is not shown by simulations with realistic boundary conditions (Kim et al. 2011; Ma and Kuang 2016).

WTG moisture mode theories of the MJO with emphasis on the warm pool mentioned above (Sobel and Maloney 2012; Sobel and Maloney 2013; Adames and Kim 2016) hold that the MJO propagation and maintenance can be explained by the evolution of moisture alone. Sobel and Maloney (2012) assume mean westerlies that produce a westward-propagating disturbance with maximum growth rate near planetary wavenumber 7. Sobel and Maloney (2013) modified this model by introducing an empirical value based on reanalysis and general circulation model (GCM) moist static budgets that is the sum of evaporation anomalies, horizontal advection, and frictionally driven boundary layer convergence. This resulted in moistening east of the convection, thus overcoming the effect of the westerly WISHE and produced eastward propagation. Adames and Kim (2016) elaborated on Sobel and Maloney (2013) by treating the meridional and vertical structure of the MJO explicitly. They adjusted several parameters and produced disturbances with more realistic characteristics, i.e., their phase speed is in agreement with the observations. They found that the eastward propagation of the MJO is explained through horizontal moisture advection, frictional convergence, and modulation of surface fluxes. Adames and Kim (2016) find that the cloud-radiative feedback at the MJO time scale is the main driver of instability while moisture advection is the primary propagation mechanism. The propagation mechanism also results in a westward group velocity.

We hold that cloud–radiation interactions (CRI) are important in MJO physics. The CRI mechanism states that deep clouds block OLR, so that the radiative cooling rate is smaller in cloudy regions than in clear ones (Albrecht and Cox 1975). Cloud–radiation interactions were shown to be of potentially great significance to large-scale motions in the tropics (Slingo and Slingo 1988; Slingo and Slingo 1991; Randall et al. 1989; Sherwood et al. 1994; Raymond 2000b, 2001; Bony and Emanuel 2005; and others). Via the CRI mechanism, the net effect of radiation reinforces the existing upward motion, which further enhances precipitation. Clear regions reinforce downward motion.

Section 2 reviews the FR and KE theories and presents a derivation of "minimal difference" models. Results for "minimal difference" models are discussed in section 3, while conclusions are given in section 4.

2. Analytical models

The governing equations of atmospheric flow for the moist atmosphere are the momentum equation, the mass continuity equation, and thermodynamic equations:

$$\frac{d\mathbf{v}}{dt} = -\frac{1}{\rho}\nabla p - 2\boldsymbol{\Omega}\times\mathbf{v} + \mathbf{g} + \frac{1}{\rho}\mathbf{F}, \tag{1}$$

$$\frac{d\rho}{dt} + \rho\nabla\cdot\mathbf{v} = 0, \tag{2}$$

$$\frac{ds}{dt} = S, \tag{3}$$

$$\frac{ds_m}{dt} = S_m. \tag{4}$$

In these equations $\mathbf{v} = (u, v, w)$ is fluid velocity field, ρ is the mass density, p is the pressure, $\mathbf{\Omega}$ is Earth's rotation vector, while $\mathbf{g}$ is gravity, the sum of gravitational and centripetal accelerations. $\mathbf{F}$ is any other force that can act on the flow. In the thermodynamic equations, s is the dry entropy with S being its source and sink term and s_m is the moist entropy with source and sink term S_m. In the simplest form dry entropy is defined as $s = C_p \ln(\theta/\theta_0)$ and moist entropy as $s_m = C_p \ln(\theta/\theta_0)$ where θ is the potential temperature, θ_e is the equivalent potential temperature, C_p is the specific heat of dry air at constant pressure, and θ_0 is a reference temperature. For full definitions of entropies and their source terms see Raymond (2013).

We now linearize (1)–(4) about a mean easterly flow and apply the hydrostatic and Boussinesq approximations. We assume that there are no other forces acting on the flow: $\mathbf{F} = 0$. Last we assume that all our variables have first baroclinic mode structure with a rigid lid: $(u, v, p) \sim \cos(mz)$, $(w, s, s_m, S, S_m) \sim \sin(mz)$ where $m = \pi/h$ is a vertical wavenumber and h is the depth of the troposphere. More complex vertical structure can be introduced, but Fuchs et al. (2012) show that adding the complexity does not influence the MJO mode. All equations are nondimensionalized with nondimensionalization given in the appendix:

$$\frac{\partial u}{\partial t} - yv - \frac{\partial s}{\partial x} = 0, \tag{5}$$

$$\frac{\partial v}{\partial t} + \delta\left(yu - \frac{\partial s}{\partial y}\right) = 0, \tag{6}$$

$$\frac{\partial u}{\partial x} + \frac{\partial v}{\partial y} + w = 0, \tag{7}$$

$$\frac{\partial s}{\partial t} + w = S, \tag{8}$$

$$\frac{\partial s_m}{\partial t} + \Gamma w = S_m. \tag{9}$$

Note that we used the linearized hydrostatic equation to relate pressure perturbation p and dry entropy s in Eqs. (5) and (6). δ is a parameter that defines the degree of zonal geostrophy defined in Table 1. Γ is the nondimensional gross moist stability parameter chosen to be positive: $\Gamma = 0.1$. Gross moist stability is a nondimensional measure of the response of vertically integrated moist static energy or moist entropy to large-scale vertical advection in a column. If it is positive, it means that an initial moisture anomaly will decay unless there are other effects. We use positive GMS as it has been shown that the instability due to negative GMS appears to be a mesoscale, or at most a synoptic-scale phenomenon (Sakaeda and Roundy 2016; Fuchs and Raymond 2017; Inoue et al. 2020).

In the original KE model x was nondimensionalized using the mean radius of Earth a. Here we have adjusted the equations in the FR model by using the same nondimensionalization as KE in x. Note that this changes values of the original FR nondimensional parameters. One of the scaling differences between the KE and FR model that is still present comes through different time scaling. KE use $T_{\mathrm{KE}}^{-1} = \beta L_y^2/a$ to nondimensionalize time, while FR use $T_{\mathrm{FR}}^{-1} = \sqrt{\beta c}$, where β is the meridional gradient of the Coriolis parameter at the equator, L_y is the meridional length scale defined in the appendix, and $c = 48\ \mathrm{m\ s^{-1}}$ is the free gravity wave speed. This time conversion leads to the following relationships between the dimensional ω and nondimensional Ω: for the FR model: $\omega = 0.65\ \mathrm{day^{-1}}\ \Omega$ and for the KE model $\omega = 0.42\ \mathrm{day^{-1}}\ \Omega$ for particular choice of some dimensional parameters. See the appendix for more information on scaling and nondimensionalization.

The momentum and mass continuity equations of FR and KE are identical though they were originally arrived at using somewhat different reasoning. KE assume that the temperature lapse rate is always moist adiabatic, which filters all but the barotropic and first baroclinic modes while FR assume first baroclinic mode structure at the outset. The barotropic mode was neglected in both models. The differences between these models arise from different treatments of moist convection and cloud–radiation interaction. FR assume that precipitation and the associated latent heating are proportional to column moisture, while KE use a mass flux approach in which the net convective mass flux is determined through an assumption of boundary layer quasi equilibrium. Although these assumptions are quite different, they lead to similar thermodynamic equations, though with some important differences, as we shall see. Another difference is that FR assume that CRI depends on column moisture whereas KE assume that it depends on column moist entropy. The differences are subtle but do lead to slightly different forms of the linear equations.

Note that we are neglecting horizontal advection of moisture that others (Sobel and Maloney 2012, 2013; Adames and Kim 2016) found could be important, because we are comparing two models that neglected it.

a. *Fuchs and Raymond model*

The FR thermodynamic equations are

$$\frac{\partial s}{\partial t} + w = S = (\alpha + \varepsilon)(s_m - s), \tag{10}$$

$$\frac{\partial s_m}{\partial t} + \Gamma w = S_m = \Lambda u + \varepsilon(s_m - s). \tag{11}$$

The source terms in the thermodynamic equations, Eqs. (10) and (11), come from the assumptions that the heating S is a result of the precipitation and cloud–radiation interactions, while moist entropy source S_m depends on surface evaporation and cloud–radiation interactions. The precipitation perturbation is parameterized to depend on the precipitable water. FR assume that it increases linearly with the vertically integrated mixing ratio perturbation $q = s_m - s$ (Raymond 2013). This increase is proportional to a moisture relaxation rate α (Raymond 2000a). The CRI mechanism, which is known to drive self-aggregation of convection in idealized, convection-permitting models, is represented here as sources terms for both dry and moist entropy that scale with their difference, with the proportionality constant ε. Surface sensible heat

TABLE 1. Numerical values of parameters.

Dimensionless parameter	FR model	KE model	Parameters values
Planetary wavenumber	L	l	—
Frequency	Ω	Ω	Ω = 1.5-day ω, Ω = 2.4-day ω
Gross moist stability	Γ	Γ	$\Gamma = 0.1$
Moisture relaxation rate	$\alpha = \frac{4.4\tilde{\alpha}}{T_{\mathrm{FR}}^{-1}}$	—	$\alpha = 1$
Cloud–radiative feedback parameter	$\varepsilon = \frac{4.4\tilde{\varepsilon}}{T_{\mathrm{FR}}^{-1}}$	$\epsilon = \frac{\tilde{\epsilon}}{T_{\mathrm{KE}}^{-1}}$	$\varepsilon = 0.4$, $\epsilon = 0.4$
WISHE parameter	$\Lambda = \frac{4.4\tilde{\Lambda}}{T_{\mathrm{FR}}^{-1}}$	$\lambda = \frac{\tilde{\Lambda}}{T_{\mathrm{KE}}^{-1}}$	$\Lambda = -0.62$, $\lambda = -0.62$
Degree of zonal geostrophy		$\delta = (a/L_y)^2$	$\delta = 30$

flux is assumed to be zero as over the tropical oceans it is very small. Surface latent heat flux is parameterized via the WISHE mechanism wherein stronger winds increase surface latent heat fluxes. WISHE comes into the Eq. (11) via Λu, where the WISHE parameter Λ is positive for imposed mean westerlies and negative for mean easterlies. The perturbations in gustiness and boundary layer mixing ratio are neglected.

The conceptual picture behind the FR model is that surface fluxes increase moisture in a vertical column, most likely over a period of several weeks, which results in an increase of water vapor in the atmospheric column and therefore the precipitation. This increase in moisture then acts via the heating budget equation aided with cloud–radiation interactions that become more significant for a more humid, and hence cloudier environment.

To solve the system of Eqs. (5)–(9) with the help of (10) and (11) for the dispersion relations, all the variables are assumed to have the form $\exp[i(lx - \Omega t)]$ in space and time, where l is a planetary wavenumber and Ω is a dimensionless frequency, see Table 1. The dispersion relation for the FR model in the case $\upsilon = 0$ is

$$\Omega^3 + i\alpha\Omega^2 - l^2\Omega - l\Lambda(\alpha + \varepsilon) - i\left[\Gamma\alpha + \varepsilon(\Gamma - 1)\right]l^2 = 0. \tag{12}$$

For the higher meridional numbers n the dispersion relations are more complex and can be found in Fuchs and Raymond (2017).

b. *Khairoutdinov and Emanuel model*

The KE model differs from FR both in the choice of nondimensional scaling (see the appendix) and in the equations themselves. The KE thermodynamic equations are

$$\frac{\partial s}{\partial t} + w = S = \lambda u + (1 + \epsilon)(s_m - s) - \chi' s, \tag{13}$$

$$\gamma\frac{\partial s_m}{\partial t} + \Gamma w = S_m = \lambda u + \epsilon(s_m - s) - D' s + d\,\frac{\partial^2 s_m}{\partial x^2}, \tag{14}$$

where we have substituted $C \to \epsilon$, $\alpha \to -\lambda$, $\chi \to 1 + \epsilon + \chi'$, and $D \to \epsilon + D'$ from the original equations of Khairoutdinov and Emanuel (2018) to bring Eqs. (13) and (14) to closer alignment with Eqs. (10) and (11) from the FR model. This will ease the comparison between the two models. Note that the FR and KE models use the symbol s in two different ways, for the FR it is dry entropy and for the KE it is saturation entropy, but the difference is absorbed in the different scaling, see the appendix.

The nondimensional constants used by Khairoutdinov and Emanuel (2018) and Emanuel (2020) in the thermodynamic equations, Eqs. (13) and (14), with above substitution are the WISHE parameter λ, the cloud–radiation interaction parameter ϵ, damping effect of boundary layer entropy perturbations on surface fluxes χ' and D', diffusion parameter d, and scaling constant γ that accounts for the different ways that s and s_m have been scaled. In the original papers of KE model (Khairoutdinov and Emanuel 2018; Emanuel 2020) there was an additional constant κ, multiplying s_m in the second term on the left side of (14), that one of us (Emanuel) has since discovered should always be one and is therefore omitted here. Note that definitions of the WISHE and CRI parameters in the KE model (λ and ϵ) differ from the corresponding parameters in the FR model ($\Lambda$and ε) due to different scaling and parameterization and are presented using different symbols.

In comparing (13) and (14) to the FR thermodynamic equations, (10) and (11), we observe several structural differences. First, there is a term involving the zonal velocity perturbation u in (13) that is missing from (10). This is a WISHE term that arises from the convective mass flux closure used by KE: perturbations in surface wind speed increase the surface enthalpy flux, which increases the moist convective mass flux, which increases temperature. Second, the terms involving dry and moist entropy, (s and s_m) appear individually, not simply as their difference, which is the case in FR. This arises from the fact that the cloud–radiation effect, represented here by the coefficient ϵ, is here taken to be proportional to s_m rather than the column moisture, which can be expressed in terms of $s_m - s$. Also, in KE the mass flux closure has a direct dependence on s_m, with mass flux increasing as s_m increases. This is responsible for the "1" in (13). Finally, the last term in (14) is a scale-dependent damping of moist entropy and was added by KE as a rough mimic of the effect of wave radiation into the stratosphere.

Solving the system of Eqs. (5)–(9) with the help of (13) and (14) for the dispersion relations with all the variables assumed to have the form $\exp[i(lx - \Omega t)]$ in space and time, where l is a planetary wavenumber and Ω is a dimensionless frequency, see Table 1, for $v = 0$ case, leads to

$$\gamma\Omega^3 + i\big[\gamma(1 + \epsilon + \chi') + dl^2 - \epsilon\big]\Omega^2 - \big[d(1 + \epsilon + \chi')l^2 - \epsilon\chi' + \gamma(l^2 - i\lambda l) + D'(1 + \epsilon)\big]\Omega - i\big[dl^2(l^2 - i\lambda l) - \epsilon l^2 + (1 + \epsilon)\Gamma l^2 - i\lambda l\big] = 0. \quad (15)$$

For the higher meridional numbers n the dispersion relations are more complex and can be found in Emanuel (2020).

c. FR and KE "minimal difference" model

The similarities between FR and KE models come from the fact that they both rely on WISHE and CRI to drive unstable modes. The main difference is that FR assume that precipitation is proportional to column moisture, while KE make use of boundary layer quasi equilibrium, producing a contribution to the mass flux proportional to the moist entropy perturbation. If one considers the moist entropy perturbation as essentially a moisture perturbation, this difference should not lead to very different results. Another difference is that FR assume that CRI depends on column moisture whereas KE assume that it depends on column moist entropy. It is important to note that the FR system has four independent specifiable coefficients, while the KE system has eight. These differences lead to different forms of the linear thermodynamic equations.

We now wish to develop a "minimal difference" model between FR and KE models, where the two models are brought most closely into alignment without losing the main physics, i.e., the WISHE and CRI mechanisms. In comparing the two systems, we should try to separate differences that arise from different parameter choices from differences that arise from structural differences in the equations.

We note that particular parameter choices bring the structures of (13) and (14) most closely into alignment with (10) and (11), namely,

$$\gamma = 1, \quad (16)$$

$$\chi' = 0, \quad (17)$$

$$D' = 0, \quad (18)$$

$$d = 0 \quad (19)$$

in the KE system, and

$$\alpha = 1 \quad (20)$$

in the FR model. This parameter choice neglects the damping effect of boundary layer entropy perturbations on surface fluxes χ' and D', and diffusion d and sets scaling constant between s and s_m to $\gamma = 1$ in the KE model. In the FR model $\alpha = 1$ implies that the moisture relaxation rate is 0.65 day^{-1} instead of 1 day^{-1} from the original FR model.

For this particular choice of parameters, Eqs. (10) and (11) from the FR model become

$$\frac{\partial s}{\partial t} + w = (1 + \varepsilon)(s_m - s), \quad (21)$$

$$\frac{\partial s_m}{\partial t} + \Gamma w = \Lambda u + \varepsilon(s_m - s) \quad (22)$$

and Eqs. (13) and (14) from the KE model become

$$\frac{\partial s}{\partial t} + w = \lambda u + (1 + \epsilon)(s_m - s), \quad (23)$$

$$\frac{\partial s_m}{\partial t} + \Gamma w = \lambda u + \epsilon(s_m - s). \quad (24)$$

Equations (23) and (24) are structurally almost identical to (21) and (22) with the only difference in an additional term, the first term, on the right-hand side of (23). This WISHE term arises from the convective mass flux closure used by KE.

The dispersion relations for the FR and KE "minimal difference" models in the case $v = 0$ are

$$\Omega^3 + i\Omega^2 - l^2\Omega - l\Lambda(1 + \varepsilon) - i\big[\Gamma + \varepsilon(\Gamma - 1)\big]l^2 = 0, \quad (25)$$

$$\Omega^3 + i\Omega^2 + (il\lambda - l^2)\Omega - l\lambda - i\big[\Gamma + \epsilon(\Gamma - 1)\big]l^2 = 0, \quad (26)$$

respectively. If $\Lambda = \lambda = 0$, i.e., in the case with no WISHE they become structurally identical. Note that different time scaling in FR and KE leads to different relationships between the nondimensional and dimensional parameters used in the FR and KE models. Those are given in Table 1, where $\tilde{\alpha}$, $\tilde{\varepsilon}$, and $\tilde{\Lambda}$ are dimensional parameters.

We shall explore the differences between the FR and KE systems for this "minimal difference" case for the eastward-propagating MJO-like mode.

3. Results

We present the results for the FR and KE "minimal difference" models for $v = 0$ or $n = -1$ case as well as for higher meridional numbers n for the same nondimensional parameters, given in Table 1: $\Gamma = 0.1$, the WISHE parameter $\Lambda = \lambda = -0.62$ and the CRI parameter $\varepsilon = \epsilon = 0.4$. The reader is invited to further explore the parameter space of both models.[1]

Figure 1 shows the eastward-propagating MJO-like mode nondimensional phase speed in the top plot, and nondimensional growth rate in the bottom plot as a function of planetary wavenumber. The red line shows results obtained from the dispersion relation (25) for the FR model. The blue line shows results obtained from the dispersion relation (26) for the KE model. The phase speeds and growth rates of the modes are fairly similar. Most importantly, both models have the highest instability at planetary wavenumber $l = 1$. Without WISHE ($\Lambda = \lambda = 0$), the modes from FR and KE model are identical, stationary with the same growth rate at all wavenumbers. Without the CRI mechanism ($\varepsilon = \epsilon = 0$), the modes from both models are unstable only for the planetary

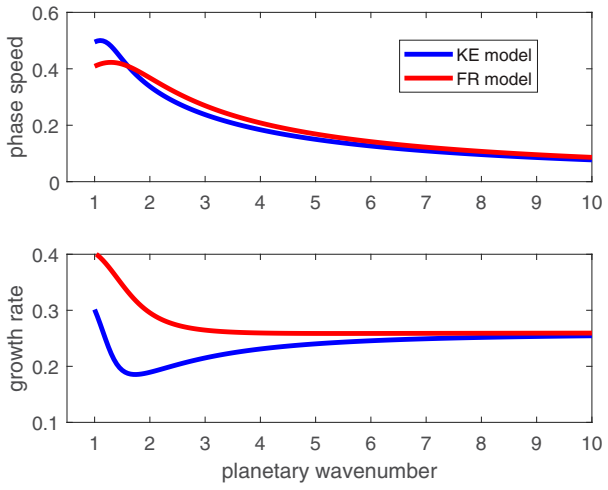

FIG. 1. (top) Eastward-propagating MJO-like mode phase speed, and (bottom) growth rate for $\upsilon = 0$ case as a function of planetary wavenumber for the FR model (red) and the KE model (blue).

wavenumber $l = 1$. WISHE is therefore responsible for eastward propagation, while both WISHE and CRI produce instability. However, WISHE is needed to produce maximum instability at planetary wavenumber $l = 1$. Note that the CRI results in instability for all wavelengths. Yano and Emanuel (1991) found that replacing the rigid lid assumption by a realistic stratosphere has the effect of strongly damping the short waves.

The explanation for the phase speed for $l = 1$ being larger than the observed OLR propagation speeds over the warm pool for both analytical models (ω/k = 15–18 m s^{-1}, $k = l/a$) was given in Raymond and Fuchs (2018). In that paper, a simple linear superposition of the warm pool rainfall and the rain from the eastward-propagating WISHE-moisture mode led to a pattern of combined rainfall moving eastward with a speed of order 5 m s^{-1}. The resulting westerly wind burst started to the west of the rainfall maximum, but ended up overrunning it as the MJO progressed across the warm pool. The strongest values of surface evaporation occurred to the east of rainfall, with an enhancement in evaporation as the MJO moved over the warm pool.

Figure 2 shows solutions of the dispersion relations for the FR "minimal difference" model and KE "minimal difference" model with the same nondimensionalized parameters given in Table 1 (WISHE and CRI included) for $n = -1$ as well as for the higher meridional numbers $n = 1, 2, 3$ for eastward- and westward-propagating unstable modes. Figure 2 shows the similarities of FR and KE "minimal difference" models across a span of zonal wavenumber and meridional mode number. KE growth rates are a little smaller at low wavenumber but do not fall off as fast with wavenumber, owing to the fact that WISHE affects the dry as well as moist entropy budgets. Across all meridional numbers the greatest instability is at the planetary wavenumber $l = 1$ for the eastward-propagating mode, giving us confidence that it represents the MJO mode. KE frequencies are a little bigger than FR ones at low wavenumber. The westward-propagating mode is the Rossby wave as seen by Fuchs-Stone et al. (2019) and Emanuel (2020).

Figure 3 shows the wave structure for $n = 1, l = 1$ case with convergent winds along the equator, in phase with the vertical velocity and a quadruple vortex structure in entropy. This figure is similar to Fig. 3 from Emanuel (2020) and is in good agreement with Fig. 2a from Hendon and Liebmann (1994) and Fig. 2 from Kiladis et al. (2005).

4. Conclusions

The value of analytical models is that they are able to clearly investigate and identify the physical mechanisms behind modeled weather disturbances. In a complex environment such as the tropical atmosphere this task is not easy. Decades of research have led the authors to narrow their focus to two models that seem to capture the essential physics behind the largest weather disturbance on our planet: the MJO. These are also highly consistent in their behavior with cloud-permitting simulations (Khairoutdinov and Emanuel 2018).

Unlike many convectively coupled waves, such as Kelvin and Rossby waves, the MJO has no analog in the dry atmosphere, which makes the starting point of research more complex. The diabatic sources that govern the heating and/or moisture budget were sought in order to model the mode that slowly propagates eastward and has the greatest instability at planetary wavenumber one as required by observations of the MJO. In this paper we present two models that accomplish this task: the FR model and the KE model. The FR model originates with Fuchs and Raymond (2002), who first modeled the moisture mode. The KE model was developed from Emanuel (1987), in which the idea of WISHE was introduced. Not until three decades later did it capture the global character of the MJO by also accounting for the effects of cloud–radiation interactions.

The FR and KE models have different parameterizations of convection. While they both include the WISHE and CRI mechanisms in their closure, the way WISHE is included is different. The FR model uses a moisture budget equation to parameterize the effect of surface fluxes, while the KE model directly parameterizes surface fluxes and precipitation efficiency into the heating budget equation. The KE model also includes damping effects of boundary layer entropy perturbations on surface fluxes and Fickian diffusion, which the FR model lacks.

In this paper, we have developed "minimal difference" models from FR and KE models, the ones that closest align to each other. The motivation behind this paper is to find a common framework between the two MJO theories, the WISHE-moisture mode theory (FR model) and the BLQE theory (KE) model. The value of this common framework is to bring two theories closer together to advance our understanding of the MJO.

The dispersion relations and their solutions for "minimal difference" FR and KE models show remarkable similarities for the $\upsilon = 0$ case as well as for higher meridional numbers.

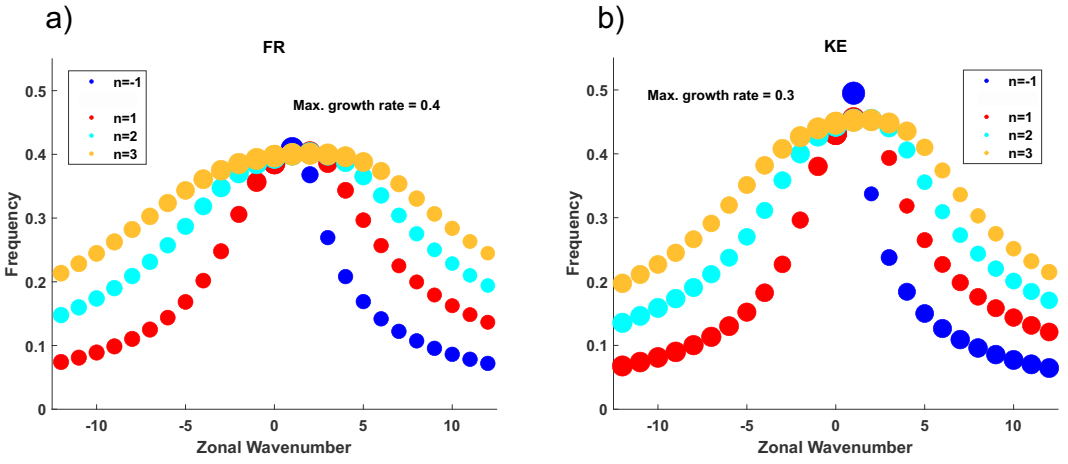

FIG. 2. Solutions of the dispersion relation for (a) the FR model and (b) the KE model. Diameters of the circles are proportional to the growth rates.

Both models obtain the eastward-propagating mode when WISHE and CRI are included, they both exhibit the greatest instability for largest wavelengths and their eigenfunctions agree with the observed horizontal structure of the MJO. The phase speeds for largest wavelengths are larger than the observed OLR speeds over the warm pool. However, Raymond and Fuchs (2018) offer an explanation for that: when the eastward-propagating mode from FR model is combined with the warm pool rainfall via linear superposition the combined pattern leads to phase speed on the order of 5 m s^{-1}.

Much of Fuchs and Raymond's previous analytical model work focused on the $v = 0$ case, which does not account for the observed meridional flows associated with the MJO. The more recent work discussed in this paper rectifies this by showing that CRI makes possible unstable $n = 1$ solutions which exhibit meridional flow. Unchanged with this extension is the global scale of the modes and the role of WISHE in their eastward propagation.

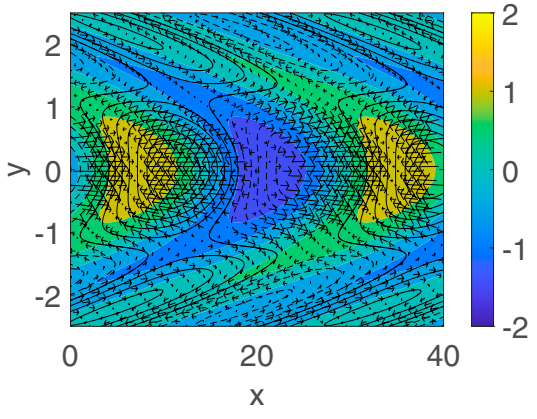

FIG. 3. Eigenfunction of the $n = 1$, $l = 1$ mode for the FR minimal difference model. The colors show the vertical velocity, the arrows show the low-level perturbations horizontal winds, and the black contours show the distribution of entropy.

The FR and KE theories do not explain the multiscale structure of the MJO or its seasonal cycle. They do not include the roles of nonlinear effects, strong mean westerlies at certain longitudes, or horizontal moisture advection. The FR and KE models formulate WISHE assuming mean planetary easterlies while many other studies focus on the fact that there are mainly westerlies present in the warm pool region. Fuchs and Raymond (2017) reported that incorporating the horizontal advection of moisture in their model did not lead to major modifications in their results. This might be because of the differences in the model setups between WTG moisture models and the FR model. It is interesting to note that both FR and KE theories as well as the WTG moisture-mode theory predict a westward group velocity of the MJO in agreement with Janiga et al. (2018), but in disagreement with some studies based on observations (Chen and Wang 2018). For more discussion and observational evidence of MJO westward group velocity see Adames and Kim (2016).

In spite of their differences both the FR and KE theories rely on tropical mean easterly low-level flows that make the WISHE mechanism possible together with cloud–radiation interactions. Both theories thus provide maximally simplified models of the MJO that agree well with observations and cloud-permitting simulations. Further evaluation is needed from observations and GCMs.

Acknowledgments. We thank David Raymond for valuable conversations and insightful comments. Željka Fuchs-Stone was supported by the NSF Grant AGS-2034817 to NMT. Kerry Emanuel was supported by the NSF Grant AGS-1906768 to MIT.

APPENDIX

FR and KE Model Nondimensionalization

Here we show nondimensionalization and scaling for the variables in FR and KE models used in Eqs. (5)–(9). Mean

radius of Earth is a while β is the meridional gradient of the Coriolis parameter at the equator.

a. FR model

Dimensional quantities are given on the left and their nondimensional equivalents are given on the right:

$$x \to ax, \tag{A1}$$

$$y \to ay, \tag{A2}$$

$$z \to \frac{1}{m} z, \tag{A3}$$

$$t \to \frac{1}{\sqrt{\beta c}} t, \tag{A4}$$

$$u \to a\sqrt{\beta c} u, \tag{A5}$$

$$v \to a\sqrt{\beta c} v, \tag{A6}$$

$$w \to \frac{\sqrt{\beta c}}{m} w, \tag{A7}$$

$$s \to ma^2 \beta c s, \tag{A8}$$

$$s_m \to ma^2 \beta c s_m, \tag{A9}$$

where c is the speed of free gravity waves and $m = \pi/h$ is a vertical wavenumber with h the depth of the troposphere.

b. KE model

As in FR model dimensional quantities are given on the left and their nondimensional equivalents are given on the right:

$$x \to ax, \tag{A10}$$

$$y \to L_y y, \tag{A11}$$

$$t \to \frac{a}{\beta L_y^2} t, \tag{A12}$$

$$u \to \frac{aC_k|\overline{\mathbf{V}}|}{H} u, \tag{A13}$$

$$v \to \frac{L_y C_k|\overline{\mathbf{V}}|}{H} v, \tag{A14}$$

$$w \to C_k|\overline{\mathbf{V}}| w, \tag{A15}$$

$$s \to \frac{aC_k|\overline{\mathbf{V}}|\beta L_y^2}{H(T_s - \overline{T})} s, \tag{A16}$$

$$s_m \to \frac{1 - \epsilon_p}{\epsilon_o} \frac{(\overline{s} - \overline{s}_m)^2}{s_0 - \overline{s}} s_m, \tag{A17}$$

where the meridional length scale is

$$L_y^4 \equiv \frac{\Gamma_d}{\Gamma_m} \frac{d\overline{s}_d}{dz} (T_s - \overline{T}) H \frac{1 - \varepsilon_p}{\beta^2}. \tag{A18}$$

In the above equations, C_k is the surface enthalpy exchange coefficient, H is a representative half depth of the troposphere, $|\overline{\mathbf{V}}|$ is the magnitude of the mean state surface winds, T_s is the surface temperature, $\overline{T}$ is the pressure-weighted vertical mean temperature of the free troposphere, ϵ_p is the bulk precipitation efficiency, s_0 is the saturation entropy of the sea surface, $\overline{s}$ is the mean state dry entropy and $\overline{s}_m$ is the mean state moist entropy, Γ_d is dry adiabatic lapse rate and Γ_m is moist adiabatic lapse rate, and $d\overline{s}_d/dz$ is static stability.

REFERENCES

Adames, Á. F., and D. Kim, 2016: The MJO as a dispersive, convectively coupled moisture wave: Theory and observations. *J. Atmos. Sci.*, **73**, 913–941, https://doi.org/10.1175/JAS-D-15-0170.1.

——, and E. D. Maloney, 2021: Moisture mode theory's contribution to advances in our understanding of the Madden-Julian oscillation and other tropical disturbances. *Curr. Climate Change Rep.*, **7**, 72–85, https://doi.org/10.1007/s40641-021-00172-4.

Albrecht, B., and S. K. Cox, 1975: The large-scale response of the tropical atmosphere to cloud modulated infrared heating. *J. Atmos. Sci.*, **32**, 16–24, https://doi.org/10.1175/1520-0469(1975)032<0016:TLSROT>2.0.CO;2.

Bony, S., and K. A. Emanuel, 2005: On the role of moist processes in tropical intraseasonal variability: Cloud–radiation and moisture–convection feedbacks. *J. Atmos. Sci.*, **62**, 2770–2789, https://doi.org/10.1175/JAS3506.1.

Chen, G., and B. Wang, 2018: Does the MJO have a westward group velocity? *J. Climate*, **31**, 2435–2443, https://doi.org/10.1175/JCLI-D-17-0446.1.

de Szoeke, S. P., J. B. Edson, J. R. Marion, C. W. Fairall, and L. Bariteau, 2015: The MJO and air–sea interaction in TOGA COARE and DYNAMO. *J. Climate*, **28**, 597–622, https://doi.org/10.1175/JCLI-D-14-00477.1.

Emanuel, K. A., 1987: An air–sea interaction model of intraseasonal oscillations in the tropics. *J. Atmos. Sci.*, **44**, 2324–2340, https://doi.org/10.1175/1520-0469(1987)044<2324:AASIMO>2.0.CO;2.

——, 2020: Slow modes of the equatorial waveguide. *J. Atmos. Sci.*, **77**, 1575–1582, https://doi.org/10.1175/JAS-D-19-0281.1.

Fuchs-Stone, Ž., 2020: WISHE-moisture mode in a vertically resolved model. *J. Adv. Model. Earth Syst.*, **12**, e2019MS001839, https://doi.org/10.1029/2019MS001839.

——, and D. J. Raymond, 2002: Large-scale modes of a nonrotating atmosphere with water vapor and cloud–radiation feedbacks. *J. Atmos. Sci.*, **59**, 1669–1679, https://doi.org/10.1175/1520-0469(2002)059<1669:LSMOAN>2.0.CO;2.

——, and ——, 2005: Large-scale modes in a rotating atmosphere with radiative–convective instability and WISHE. *J. Atmos. Sci.*, **62**, 4084–4094, https://doi.org/10.1175/JAS3582.1.

——, and ——, 2017: A simple model of intraseasonal oscillations. *J. Adv. Model. Earth Syst.*, **9**, 1195–1211, https://doi.org/10.1002/2017MS000963.

——, S. Gjorgjievska, and D. J. Raymond, 2012: Effects of varying the shape of the convective heating profile on convectively coupled gravity waves and moisture modes. *J. Atmos. Sci.*, **69**, 2505–2519, https://doi.org/10.1175/JAS-D-11-0308.1.

——, D. J. Raymond, and S. Sentić, 2019: A simple model of convectively coupled equatorial Rossby waves. *J. Adv. Model.*

Earth Syst., **11**, 173–184, https://doi.org/10.1029/2018MS001433.

Hayashi, M., and H. Itoh, 2017: A new mechanism of the slow eastward propagation of unstable disturbances with convection in the tropics: Implications for the MJO. *J. Atmos. Sci.*, **74**, 3749–3769, https://doi.org/10.1175/JAS-D-16-0300.1.

Hendon, H. H., and B. Liebmann, 1994: Organization of convection within the Madden-Julian oscillation. *J. Geophys. Res.*, **99**, 8073–8083, https://doi.org/10.1029/94JD00045.

Inoue, K., Á. F. Adames, and K. Yasunaga, 2020: Vertical velocity profiles in convectively coupled equatorial waves and MJO: New diagnoses of vertical velocity profiles in the wavenumber–frequency domain. *J. Atmos. Sci.*, **77**, 2139–2162, https://doi.org/10.1175/JAS-D-19-0209.1.

Janiga, M. A., C. J.Schreck III, J. A. Ridout, M. Flatau, N. P. Barton, E. J. Metzger, and C. A. Reynolds, 2018: Subseasonal forecasts of convectively coupled equatorial waves and the MJO: Activity and predictive skill. *Mon. Wea. Rev.*, **146**, 2337–2360, https://doi.org/10.1175/MWR-D-17-0261.1.

Jiang, X., and Coauthors, 2020: Fifty years of research on the Madden-Julian oscillation: Recent progress, challenges, and perspectives. *J. Geophys. Res. Atmos.*, **125**, e2019JD030911, https://doi.org/10.1029/2019JD030911.

Khairoutdinov, M. F., and K. Emanuel, 2018: Intraseasonal variability in a cloud-permitting near-global equatorial aquaplanet model. *J. Atmos. Sci.*, **75**, 4337–4355, https://doi.org/10.1175/JAS-D-18-0152.1.

Kiladis, G. N., K. H. Straub, and P. T. Haertel, 2005: Zonal and vertical structure of the Madden–Julian oscillation. *J. Atmos. Sci.*, **62**, 2790–2809, https://doi.org/10.1175/JAS3520.1.

——, M. C. Wheeler, P. T. Haertel, K. H. Straub, and P. E. Roundy, 2009: Convectively coupled equatorial waves. *Rev. Geophys.*, **47**, RG2003, https://doi.org/10.1029/2008RG000266.

Kim, D., A. H. Sobel, and I. S. Kang, 2011: A mechanism denial study on the Madden Julian oscillation. *J. Adv. Model. Earth Syst.*, **3**, M12007, https://doi.org/10.1029/2011MS000081.

Kiranmayi, L., and E. D. Maloney, 2011: Intraseasonal moist static energy budget in reanalysis data. *J. Geophys. Res.*, **116**, D21117, https://doi.org/10.1029/2011JD016031.

Kuang, Z., 2008: A moisture-stratiform instability for convectively coupled waves. *J. Atmos. Sci.*, **65**, 834–854, https://doi.org/10.1175/2007JAS2444.1.

Li, T., L. Wang, M. Peng, and B. Wang, 2018: A paper on the tropical intraseasonal oscillation published in 1963 in a Chinese journal. *Bull. Amer. Meteor. Soc.*, **99**, 1765–1779, https://doi.org/10.1175/BAMS-D-17-0216.1.

Ma, D., and Z. Kuang, 2016: A mechanism-denial study on the Madden-Julian oscillation with reduced interference from mean statechanges. *Geophys. Res. Lett.*, **43**, 2989–2997, https://doi.org/10.1002/2016GL067702.

Madden, R. A., and P. R. Julian, 1971: Detection of a 40–50 day oscillation in the zonal wind in the tropical Pacific. *J. Atmos. Sci.*, **28**, 702–708, https://doi.org/10.1175/1520-0469(1971)028<0702:DOADOI>2.0.CO;2.

Majda, A. J., and S. N. Stechmann, 2009: A simple dynamical model with features of convective momentum transport. *J. Atmos. Sci.*, **66**, 373–392, https://doi.org/10.1175/2008JAS2805.1.

Matsuno, T., 1966: Quasi-geostrophic motions in the equatorial area. *J. Meteor. Soc. Japan*, **44**, 25–43, https://doi.org/10.2151/jmsj1965.44.1_25.

Neelin, J. D., I. M. Held, and K. H. Cook, 1987: Evaporation–wind feedback and low-frequency variability in the tropical atmosphere. *J. Atmos. Sci.*, **44**, 2341–2348, https://doi.org/10.1175/1520-0469(1987)044<2341:EWFALF>2.0.CO;2.

Peixoto, J. P., and A. H. Oort, 1992: *Physics of Climate*. American Institute of Physics, 520 pp.

Randall, D., A. Harshvardhan, D. A. Dazlich, and T. G. Corsetti, 1989: Interactions among radiation, convection, and large-scale dynamics in a general circulation model. *J. Atmos. Sci.*, **46**, 1943–1970, https://doi.org/10.1175/1520-0469(1989)046<1943:IARCAL>2.0.CO;2.

Raymond, D. J., 2000a: Thermodynamic control of tropical rainfall. *Quart. J. Roy. Meteor. Soc.*, **126**, 889–898, https://doi.org/10.1002/qj.49712656406.

——, 2000b: The Hadley circulation as a radiative–convective instability. *J. Atmos. Sci.*, **57**, 1286–1297, https://doi.org/10.1175/1520-0469(2000)057<1286:THCAAR>2.0.CO;2.

——, 2001: A new model of the Madden–Julian oscillation. *J. Atmos. Sci.*, **58**, 2807–2819, https://doi.org/10.1175/1520-0469(2001)058<2807:ANMOTM>2.0.CO;2.

——, 2013: Sources and sinks of entropy in the atmosphere. *J. Adv. Model. Earth Syst.*, **5**, 755–763, https://doi.org/10.1002/jame.20050.

——, and Ž. Fuchs, 2007: Convectively coupled gravity and moisture modes in a simple atmospheric model. *Tellus*, **59**, 627–640, https://doi.org/10.1111/j.1600-0870.2007.00268.x.

——, and ——, 2018: The Madden-Julian oscillation and the Indo-Pacific warm pool. *J. Adv. Model. Earth Syst.*, **10**, 951–960, https://doi.org/10.1002/2017MS001258.

Rostami, M., and V. Zeitlin, 2019: Eastward-moving convection-enhanced modons in shallow water in the equatorial tangent plane. *Phys. Fluids*, **31**, 021701, https://doi.org/10.1063/1.5080415.

Sakaeda, N., and P. E. Roundy, 2016: Gross moist stability and the Madden–Julian oscillation in reanalysis data. *Quart. J. Roy. Meteor. Soc.*, **142**, 2740–2757, https://doi.org/10.1002/qj.2865.

Sentić, S., Ž. Fuchs-Stone, and D. J. Raymond, 2020: The Madden-Julian oscillation and mean easterly winds. *J. Geophys. Res. Atmos.*, **125**, e2019JD030869, https://doi.org/10.1029/2019JD030869.

Sherwood, S. C., V. Ramanathan, T. P. Barnett, M. K. Tyree, and E. Roeckner, 1994: Response of an atmospheric general circulation model to radiative forcing of tropical clouds. *J. Geophys. Res.*, **99**, 20 829–20 845, https://doi.org/10.1029/94JD01632.

Shi, X., D. Kim, F. Adames, and J. Sukhatme, 2018: WISHE-moisture mode in an aquaplanet simulation. *J. Adv. Model. Earth Syst.*, **10**, 2393–2407, https://doi.org/10.1029/2018MS001441.

Slingo, A., and J. M. Slingo, 1988: The response of a general circulation model to cloud longwave radiative forcing. I: Introduction and initial experiments. *Quart. J. Roy. Meteor. Soc.*, **114**, 1027–1062, https://doi.org/10.1002/qj.49711448209.

Slingo, J. M., and A. Slingo, 1991: The response of a general circulation model to cloud longwave radiative forcing. II: Further studies. *Quart. J. Roy. Meteor. Soc.*, **117**, 333–364, https://doi.org/10.1002/qj.49711749805.

Sobel, A., and E. Maloney, 2012: An idealized semi-empirical framework for modeling the Madden–Julian oscillation. *J. Atmos. Sci.*, **69**, 1691–1703, https://doi.org/10.1175/JAS-D-11-0118.1.

——, and ——, 2013: Moisture modes and the eastward propagation of the MJO. *J. Atmos. Sci.*, **70**, 187–192, https://doi.org/10.1175/JAS-D-12-0189.1.

——, S. Wang, and D. Kim, 2014: Moist static energy budget of the MJO during DYNAMO. *J. Atmos. Sci.*, **71**, 4276–4291, https://doi.org/10.1175/JAS-D-14-0052.1.

Thual, S., A. J. Majda, and S. N. Stechmann, 2014: A stochastic skeleton model for the MJO. *J. Atmos. Sci.*, **71**, 697–715, https://doi.org/10.1175/JAS-D-13-0186.1.

Wang, B., and H. Rui, 1990: Dynamics of the coupled moist Kelvin–Rossby wave on an equatorial beta-plane. *J. Atmos. Sci.*, **47**, 397–413, https://doi.org/10.1175/1520-0469(1990)047<0397:DOTCMK>2.0.CO;2.

——, F. Liu, and G. Chen, 2016: A trio-interaction theory for Madden–Julian oscillation. *Geosci. Lett.*, **3**, 34, https://doi.org/10.1186/s40562-016-0066-z.

Wheeler, M., and G. N. Kiladis, 1999: Convectively coupled equatorial waves: Analysis of clouds and temperature in the wavenumber–frequency domain. *J. Atmos. Sci.*, **56**, 374–399, https://doi.org/10.1175/1520-0469(1999)056<0374:CCEWAO>2.0.CO;2.

Xie, Y.-B., S.-J. Chen, I.-L. Zhang, and Y.-L. Hung, 1963: A preliminarily statistic and synoptic study about the basic currents over southeastern Asia and the initiation of typhoon (in Chinese). *Acta Meteor. Sin.*, **33**, 206–217.

Yang, D., and A. P. Ingersoll, 2013: Triggered convection, gravity waves, and the MJO: A shallow-water model. *J. Atmos. Sci.*, **70**, 2476–2486, https://doi.org/10.1175/JAS-D-12-0255.1.

——, and ——, 2014: A theory of the MJO horizontal scale. *Geophys. Res. Lett.*, **41**, 1059–1064, https://doi.org/10.1002/2013GL058542.

Yano, J.-I., and K. A. Emanuel, 1991: An improved model of the equatorial troposphere and its coupling with the stratosphere. *J. Atmos. Sci.*, **48**, 377–389, https://doi.org/10.1175/1520-0469(1991)048<0377:AIMOTE>2.0.CO;2.

——, and J. J. Tribbia, 2017: Tropical atmospheric Madden–Julian oscillation: A strongly nonlinear free solitary Rossby wave? *J. Atmos. Sci.*, **74**, 3473–3489, https://doi.org/10.1175/JAS-D-16-0319.1.

Zhang, C., 1996: Atmospheric intraseasonal variability at the surface in the tropical western Pacific Ocean. *J. Atmos. Sci.*, **53**, 739–758, https://doi.org/10.1175/1520-0469(1996)053<0739:AIVATS>2.0.CO;2.

——, 2005: Madden-Julian oscillation. *Rev. Geophys.*, **43**, RG2003, https://doi.org/10.1029/2004RG000158.

——, 2013: Madden–Julian oscillation: Bridging weather and climate. *Bull. Amer. Meteor. Soc.*, **94**, 1849–1870, https://doi.org/10.1175/BAMS-D-12-00026.1.

——, Á. F. Adames, B. Khouider, B. Wang, and D. Yang, 2020: Four theories of the Madden-Julian oscillation. *Rev. Geophys.*, **58**, e2019RG000685, https://doi.org/10.1029/2019RG000685.